

# Investigation on nonlinear optical and dielectric properties of L-arginine doped ZTC crystal to explore photonic device applications

MOHD ANIS<sup>1</sup>, S.S. HUSSAINI<sup>2</sup>, M.D. SHIRSAT<sup>3</sup>, G.G. MULEY<sup>1,\*</sup>

<sup>1</sup>Department of Physics, Sant Gadge Baba Amravati University, Amravati-444602, Maharashtra, India

<sup>2</sup>Crystal Growth Laboratory, Department of Physics, Milliya Arts, Science and Management Science College, Beed-431122, Maharashtra, India

<sup>3</sup>Intelligent Materials Research Laboratory, Department of Physics, Dr. Babasaheb Ambedkar Marathwada University, Aurangabad-431005, Maharashtra, India

The present study is focused to explore the photonic device applications of L-arginine doped ZTC (LA-ZTC) crystals using nonlinear optical (NLO) and dielectric studies. The LA-ZTC crystals have been grown by slow evaporation solution technique. The chemical composition and surface of LA-ZTC crystal have been analyzed by means of energy dispersive spectroscopy (EDS) and surface scanning electron microscopy (SEM) techniques. The Vicker's microhardness study has been carried out to determine the hardness, work hardening index, yield strength and elastic stiffness of LA-ZTC crystal. The enhanced SHG efficiency of LA-ZTC crystal has been ascertained using the Kurtz-Perry powder SHG test. The closed-and-open aperture Z-scan technique has been employed to confirm the third order nonlinear optical nature of LA-ZTC crystal. The Z-scan transmittance data has been utilized to calculate the superior cubic susceptibility, nonlinear refractive index, nonlinear absorption coefficient and figure of merit of LA-ZTC crystal. The behavior of dielectric constant and dielectric loss of LA-ZTC crystal at different temperatures has been investigated using the dielectric analysis.

Keywords: *crystal growth; spectroscopic studies; microhardness studies; SHG efficiency test; Z-scan analysis; dielectric studies*

© Wrocław University of Technology.

## 1. Introduction

In the field of optical technology, efficient second and third order nonlinear optical (TONLO) organic and semi-organic crystals have evoked a huge demand for designing highly tuned devices for laser frequency conversion, optical power limiting, optical modulation, laser alignment, photonics and optical data storage systems [1, 2]. Amongst all the thiourea metal complexes, zinc thiourea chloride (ZTC) has been extensively studied in the past decade to enhance its properties so as it could be exploited for distinct NLO driven photonic device applications. As doping can largely influence the characteristic traits of the crystal system, various researchers have re-investigated the ZTC

crystal using different amino acids. The positive impact of glycine on structural, UV-Vis, thermal and SHG efficiency of ZTC crystal has been reported in the literature [3]. The improved structural, linear-nonlinear optical and thermal studies of L-alanine doped ZTC crystal have been explored [4]. The influence of L-cysteine on optical transparency, SHG efficiency, photoluminescence, thermal and dielectric properties of ZTC crystal has been investigated [5]. As L-arginine (LA) is a potential chiral amino acid with wide hydrogen bonding network, researchers have explored the doping effect of different mol.% of LA on morphological, nucleation, structural, optical and mechanical properties of ZTC crystal [6, 7]. Recently, we have firstly reported a significant impact of very small quantity of LA (1 wt.%) on structural, optical, dielectric, photoconductivity and thermal behavior

\*E-mail: gajanangm@yahoo.co.in

of ZTC crystal [8], which gave outstanding results as compared to other reported works. Hitherto, not a single researcher has reported the influence of LA on TONLO properties of ZTC crystal. This short communication is aimed to investigate the spectroscopic, mechanical, SHG efficiency and third order nonlinear optical and dielectric properties of 1 wt.% LA doped ZTC (LA-ZTC) crystal using SEM, EDS, microhardness, Kurtz-Perry SHG test, Z-scan and dielectric characterization techniques to explore the integrated optics and photonic device applications.



Fig. 1. Photograph of LA-ZTC crystals.

## 2. Experimental

The pure ZTC complex has been synthesized by dissolving AR grade zinc chloride and thiourea in a double distilled deionized water with a ratio of 1:2. The purity of ZTC complex was achieved by repetitive recrystallization process. The supersaturated solution of ZTC complex was prepared at room temperature and a measured quantity of 1 wt.% of LA was added to it. The mixture was allowed to stir for five hours in order to achieve the homogeneous doping of LA in ZTC complex. The solution was then filtered in a rinsed beaker using the Whatman filter paper. The filtered LA doped ZTC solution was allowed for slow

evaporation in a bath with a constant temperature of accuracy  $\pm 0.01$  °C. The optically transparent thin LA-ZTC crystals shown in Fig. 1 were harvested within the period of 3 weeks.

## 3. Results and discussion

### 3.1. EDS and SEM analysis

The chemical composition of LA-ZTC crystal has been qualitatively determined using a JEOL 6360 instrument to confirm the incorporation of LA in ZTC crystal. The compositional mass% of each element, namely carbon (C), nitrogen (N), zinc (Zn), chlorine (Cl) and oxygen (O), identified in the LA-ZTC crystal, are shown in EDS spectrum (Fig. 2a). As ZTC crystal does not possess oxygen, the presence of O with high mass% of 59.13 clearly evidences the presence of LA in ZTC crystal.

The surface of LA-ZTC crystal has been evaluated using the SEM analysis carried out with the JEOL-2300 instrument. The SEM micrograph (Fig. 2b) of selected area of LA-ZTC crystal sample has been recorded at a resolution of 100  $\mu\text{m}$  which was achieved by detecting the signals received due to the electron-surface interaction. The major area of the image is covered by intense white color substance which evidences the presence of chlorine in the sample [9]. The large multinucleations were observed on the crystal surface which might have occurred due to organic dopant LA. The absence of cracks and voids confirm the perfection of LA-ZTC crystal.

### 3.2. Microhardness studies

The Vicker's microhardness study has been done using a Shimadzu HMV-2T microhardness analyzer to assess the mechanical properties of LA-ZTC crystal. The Vicker's hardness number (VHN) of LA-ZTC crystal has been determined at different indentation loads using the relation:  $H_v = 1.8544 P/d^2$   $\text{kG/mm}^2$ , where P is the applied load in kG and d is the average indentation diagonal length in mm [10]. The VHN for each load applied for a constant period of 5 sec is plotted in Fig. 3a. It reveals that the hardness of LA-ZTC crystal increases with the applied load which confirms that the stress

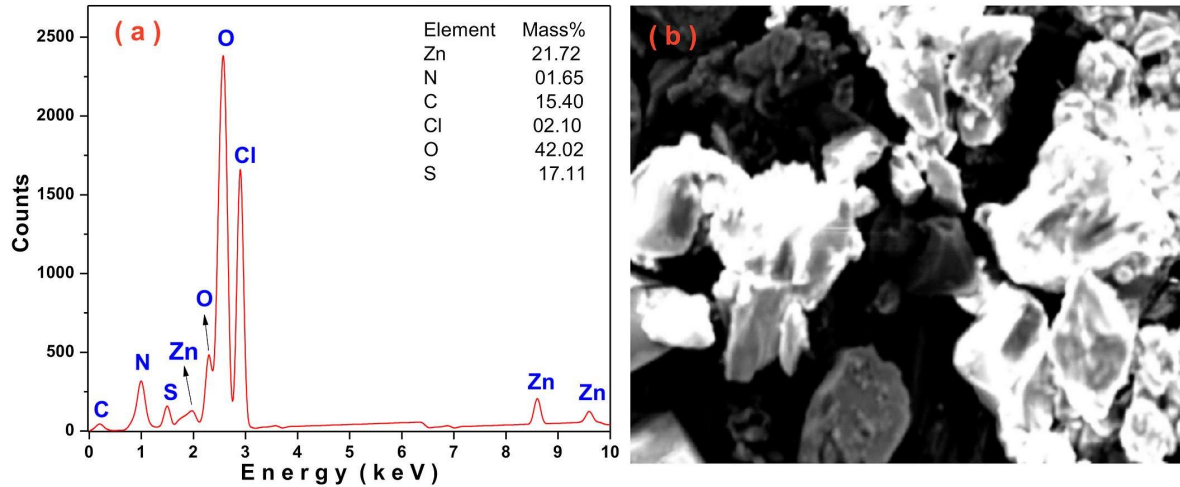


Fig. 2. (a) EDS spectrum of LA-ZTC crystal, (b) SEM micrograph of LA-ZTC crystal.

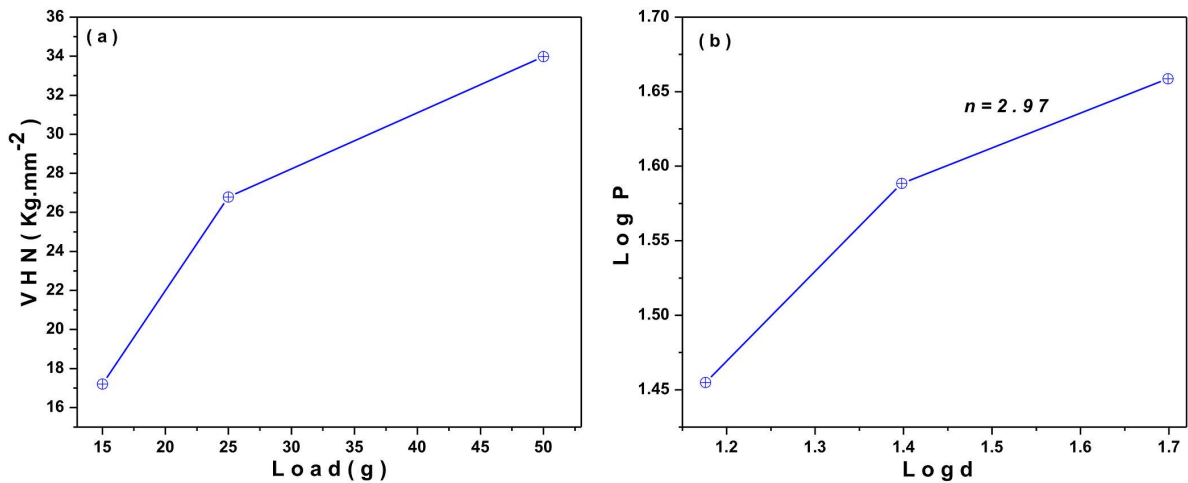


Fig. 3. (a) Load dependent hardness (b) logP vs. logd.

required for homogeneous nucleation of lattice dislocations is larger for higher load. The work hardening coefficient ( $n$ ) of material depends on the dislocation movement in the crystal system for which Meyer's law,  $P = Kd^n$  can be employed [11]. The  $n$  of LA-ZTC crystal has been determined from the slope of the plot of  $\log P$  vs.  $\log d$ , shown in Fig. 3b. The magnitude of  $n$  has been found to be 2.97, and such materials falls to the category of soft materials obeying the Onitsch criterion [12]. In proper selection of materials for high-edge mechanical device fabrication the elastic stiffness constant ( $C_{11} = H_v^{7/4}$ ) and yield strength ( $\sigma_y = (0.1)^{n-2} H_v/3$ ) play a crucial role. The calculated hardness parameters

are shown in Table 1. The increasing nature of  $C_{11}$  and  $\sigma_y$  clearly evidences the high bond strength between the neighboring atoms of LA-ZTC crystal system [13]. The good mechanical stability of LA-ZTC crystal is beneficial for avoiding breakage and wastage of material while processing for device fabrication [10, 14].

Table 1. Hardness parameters of LA-ZTC crystal.

Load [g]	VHN [kG/mm <sup>2</sup> ]	$C_{11}$ [GPa]	$\sigma_y$ [Pa]
15	17.2	$2.49 \times 10^5$	6020510
25	26.79	$5.41 \times 10^5$	9377294
50	33.98	$8.20 \times 10^5$	11894007

### 3.3. SHG efficiency test

The Kurtz-Perry powder SHG test is a decisive technique to determine the second order conversion efficiency of given material [15]. For present analysis, the single KDP and LA-ZTC crystals were powdered to micro-granules of even grain size and tightly packed in a quartz cavity. The prepared samples were multi-shot by a polarized Gaussian beam of Q-switched Nd:YAG laser operating at 1064 nm, having a pulse width of 6 ns, delivering the energy of 5.4  $\mu$ J/pulse with a repetition rate of 10 Hz. The output intensities of each sample were recorded through an array of photomultiplier tubes. The emission of bright green light at the output window confirmed the nonlinear behavior of the grown crystals. The SHG intensities of KDP and LA-ZTC crystal samples are plotted in Fig. 4. It reveals that the SHG efficiency of LA-ZTC crystal is 1.96 times higher than that of KDP crystal material. In the literature, the SHG efficiency of 1 mol.%, 3 mol.% and 5 mol.% of LA-ZTC crystal was reported to be 0.65, 0.71 and 0.75 times that of KDP crystal which is significantly lower than that of 1 wt.% LA-ZTC crystal [6]. The enhanced NLO response of LA-ZTC crystal is mainly attributed to the noncentrosymmetric complexity, wide hydrogen bonding network and enhanced photoinduced  $\pi$ -electron charge transfer through the donor-acceptor chromospheres [16]. The LA-ZTC with high SHG efficiency is highly advisable crystal for application in laser frequency conversion devices.

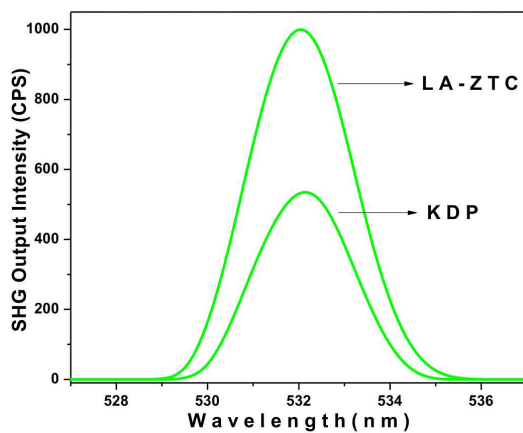


Fig. 4. Plot of SHG output intensity.

### 3.4. Z-scan analysis

Table 2. Optical resolution of Z-scan setup.

Parameters	Magnitude
Laser wavelength ( $\lambda$ )	632.8 nm
Laser power (P)	10 mW
Lens focal length (f)	20 cm
Optical path distance (Z)	113 cm
Beam waist radius ( $\omega_a$ )	1 mm
Aperture radius ( $r_a$ )	1.5 mm
Incident intensity at the focus ( $I_0$ )	2.3375 KW/m <sup>2</sup>

The Z-scan is the most sensitive and effective technique to examine and measure the third order nonlinear optical (TONLO) parameters of material [17]. In order to determine the TONLO behavior of LA-ZTC crystal, closed and open aperture Z-scan technique (Table 2) was employed using the He-Ne laser operating at 632.8 nm. The crystal sample of 1mm thickness was placed at the focus ( $Z = 0$ ) of a beam irradiated path and a polarized laser beam was concentrated on the sample through a converging lens. The crystal was translated to and fro about the focus along the Z-direction. The configuration in which the intensity transmitted by the crystal sample along the Z-directed translation is measured through a photodetector with closed aperture is defined as closed aperture Z-scan technique. The closed aperture Z-scan transmittance curve shown in Fig. 5a helps to identify the nature of nonlinear refraction (NLR) of the crystal. It reveals that the transmittance of LA-ZTC crystal offers a valley to peak phase transition about the focus, which confirms the self-focusing nature of the LA-ZTC crystal. The self-focusing nature identifies the LA-ZTC crystal as a positive NLR material [18]. The spatial distribution and localized absorption of highly repetitive optical energy along the crystal surface is the primary factor governing NLR in the crystal system [19]. The difference between the peak to valley transmittance ( $\Delta T_{p-v}$ ) in terms of on axis phase shift ( $\Delta\Phi$ ) is defined as [17]:

$$\Delta T_{p-v} = 0.406(1-S)^{0.25} |\Delta\Phi| \quad (1)$$

where  $S = [1 - \exp(-2r_a^2/\omega_a^2)]$  is the aperture linear transmittance,  $r_a$  is the aperture radius and  $\omega_a$  is

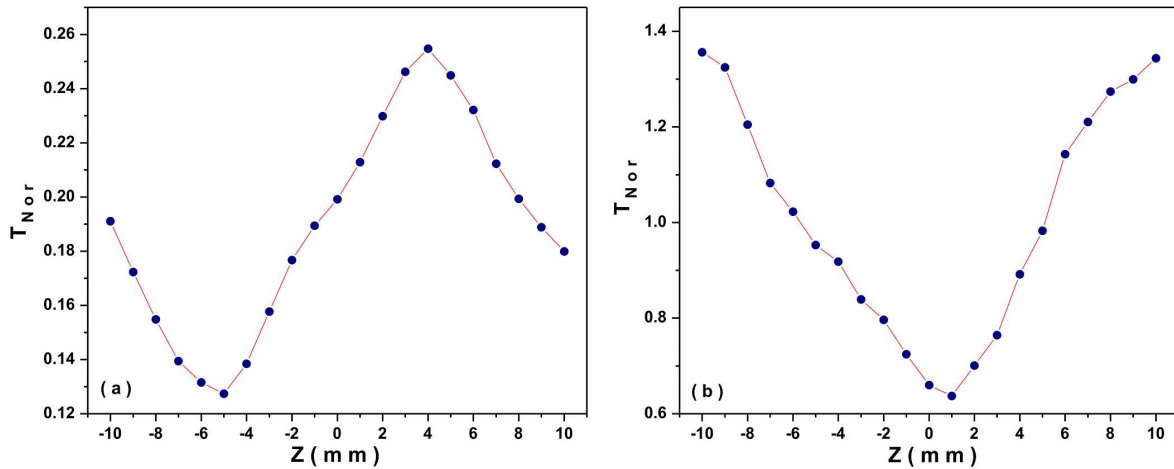


Fig. 5. Z-scan transmittance curve with (a) closed and (b) open aperture.

the beam radius at the aperture. The magnitude of NLR ( $n_2$ ) was calculated using the equation [17]:

$$n_2 = \frac{\Delta\phi}{KI_0L_{eff}} \quad (2)$$

where  $K = 2\pi/\lambda$  ( $\lambda$  is the laser wavelength),  $I_0$  is the intensity of laser beam at the focus ( $Z = 0$ ),  $L_{eff} = [1 - \exp(-\alpha L)]/\alpha$ , is the effective thickness of the sample depending on linear absorption coefficient ( $\alpha$ ) and  $L$  is the thickness of the sample. The NLR ( $n_2$ ) of LA-ZTC crystal is found to be  $4.45 \times 10^{-9} \text{ cm}^2/\text{W}$ . The high magnitude of positive NLR defines the potential ability of material to inherit Kerr lens mode locking (KLM) which is the most desirable feature for designing photonic devices, such as laser alignment systems, shorter pulse generation accessories and optical switching devices [20, 21]. The open aperture (OA) Z-scan study determines the nature and magnitude of nonlinear absorption (NLA) behavior of material. The OA Z-scan curve of LA-ZTC crystal is shown in Fig. 5b. It is observed that the transmittance along the Z-direction falls at the focus which confirms the origin of reverse saturable absorption (RSA). The RSA effect is observed due to multiphoton absorption (MPA) effect facilitated by dominance of excited state absorption over the linear absorption coefficient of crystal [22]. The LA-ZTC crystal with RSA feature is a substantial material for photonic and biomedical devices [23].

The NLA coefficient ( $\beta$ ) of crystal has been calculated from equation [17]:

$$\beta = \frac{2\sqrt{2}\Delta T}{I_0L_{eff}} \quad (3)$$

where  $\Delta T$  is the one valley value at the open aperture Z-scan curve. The  $\beta$  of LA-ZTC crystal was found to be  $8.23 \times 10^{-4} \text{ cm/W}$ . The TONLO susceptibility ( $\chi^3$ ) of material determines the merit of photoinduced polarizing ability of material [24]. The  $\chi^3$  was calculated using the following equations [17]:

$$Re\chi^3(esu) = 10^{-4}(\epsilon_0 C^2 n_0^2 n_2) / \pi (cm^2/W) \quad (4)$$

$$Im\chi^3(esu) = 10^{-2}(\epsilon_0 C^2 n_0^2 \lambda \beta) / 4\pi^2 (cm/W) \quad (5)$$

$$\chi^3 = \sqrt{(Re\chi^3)^2 + (Im\chi^3)^2} \quad (6)$$

where  $\epsilon_0$  is the vacuum permittivity,  $n_0$  is the linear refractive index of the sample and  $c$  is the velocity of light in vacuum. The  $\chi^3$  of LA-ZTC crystal was found to be of order  $10^{-3} \text{ esu}$ . The TONLO parameters of LA-ZTC crystal are comparatively collected in Table 3 [25, 26]. The figure of merit ( $T = \beta\lambda/n_2$ ) of LA-ZTC crystal was found to be 21.86. This evidences the dominance of NLR over NLA which is a vital factor for designing photonic devices [27]. The promising TONLO parameters confirm the high suitability of LA-ZTC crystal for laser and photonic devices.

Table 3. TONLO parameters of LA-ZTC crystal.

Crystal	$n_2$ [cm <sup>2</sup> /W]	$\beta$ [cm/W]	$\chi^3$ [esu]
LA-ZTC*	$4.45 \times 10^{-9}$	$8.2 \times 10^{-4}$	$2.43 \times 10^{-3}$
ZTC [24]	$-6.64 \times 10^{-8}$	$-7.25 \times 10^{-3}$	$3.6 \times 10^{-6}$
$\alpha$ -LiIO <sub>3</sub> [25]	$5.46 \times 10^{-7}$	3.95	$1.63 \times 10^{-3}$

\*Present study

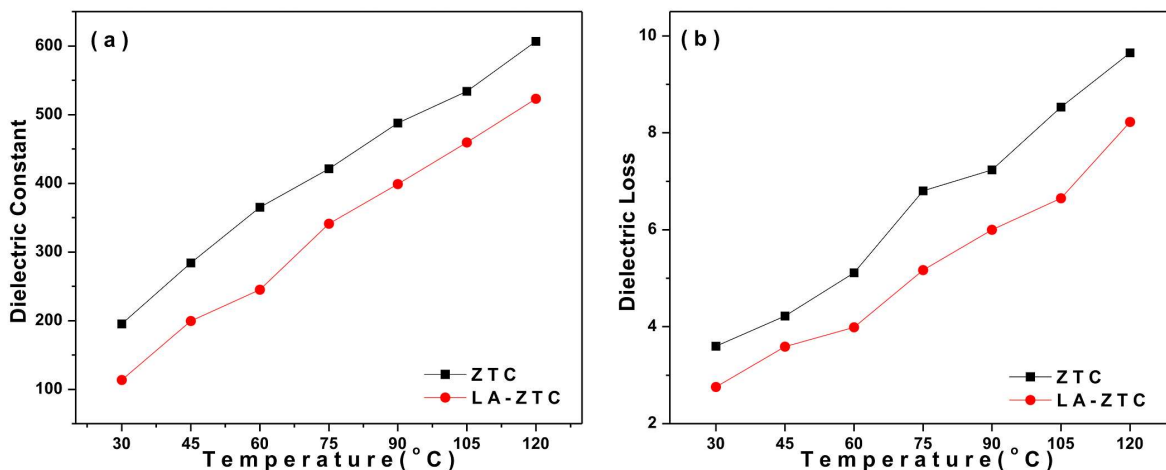


Fig. 6. Temperature dependent (a) dielectric constant, (b) dielectric loss.

### 3.5. Dielectric studies

The dielectric constant and dielectric loss of LA-ZTC crystal have been investigated in the range of 30 °C to 120 °C using a HIOKI-3532 LCR cube-meter. The sample crystal was polished and covered by silver paste on the surface to ensure good electrical contact with the LCR probe.

The dielectric properties of material are strongly influenced by the applied external frequency as well as temperature. The dielectric constants ( $\epsilon_r = Cd/\epsilon_0 A$ , where  $C$  is the capacitance of the sample,  $d$  is the thickness,  $\epsilon_0$  is the permittivity of free space and  $A$  is the area of the crystal sample) of pure and LA-ZTC crystals are shown in Fig. 6a. The dielectric constant is attributed to the electronic, ionic, dipolar and space charge polarization which increases with the rise in temperature. The increase in dielectric constant is observed as the space charge polarization is dominant at lower frequency and higher temperature [10]. It is observed that the dielectric constant of LA-ZTC

crystal is significantly lower than that of ZTC. As materials with lower dielectric constant consume less power, hence LA-ZTC crystal is superior to ZTC for designing broad-band electro-optic modulators, field detectors, photonics and microelectronics devices [28]. In Fig. 6b, the dielectric loss ( $\tan\delta = \epsilon_r/\epsilon_0$ ) of LA-ZTC crystal is observed to be lower than that of ZTC crystal which confirms its improved quality and lower defect concentration [29].

## 4. Conclusions

In present investigation, optically transparent LA-ZTC crystals have been grown at room temperature. The surface of LA-ZTC crystal has been investigated by SEM analysis. In EDS spectrum, the detection of oxygen in large quantity confirmed the incorporation of LA in ZTC crystal. The Vicker's microhardness study revealed high values of VHN, elastic stiffness and yield strength of LA-ZTC crystal for high applied loads. The work hardening coefficient was found to be 2.97.

The SHG efficiency of LA-ZTC crystal was found to be 1.96 times of that of KDP crystal material. The Z-scan confirmed promising TONLO nature of LA-ZTC crystal. The positive NLR of magnitude  $4.45 \times 10^{-9} \text{ cm}^2/\text{W}$  confirmed the strong KLM ability of LA-ZTC crystal which is desired for various laser tuning and optical switching device applications. The origin of RSA confirmed the potential usefulness of LA-ZTC crystal for photonic applications. The cubic susceptibility of LA-ZTC crystal was found to be  $2.43 \times 10^{-3}$  esu. All above studies infer that LA-ZTC crystal is highly advisable for photonic applications, namely laser tuning, frequency conversion, NLO and optical switching devices.

### Acknowledgements

The author, Mohd Anis, is thankful to the UGC for awarding the Maulana Azad Junior Research Fellowship (F1-17.1/2015-16/MANF-2015-17-MAH-68193).

### References

- [1] VANISHRI S., BABU REDDY J.N., BHAT H.L., GHOSH S., *Appl. Phys. B*, 88 (2007), 457.
- [2] RAVINDRA H.J., CHANDRASHEKARAN K., HARRISON W.T.A., DHARMAPRAKASH S.M., *Appl. Phys. B*, 94 (2009), 503.
- [3] HUSSAINI S.S., DHUMANE N.R., DONGRE V.G., SHIRSAT M.D., *J. Optoelectron. Adv. M.*, 2 (2008), 108.
- [4] DHUMANE N.R., HUSSAINI S.S., DONGRE V.G., GHUGARE P., SHIRSAT M.D., *Appl. Phys. A*, 95 (2009), 727.
- [5] ANIS M., SHAIKH R.N., SHIRSAT M.D., HUSSAINI S.S., *Opt. Laser Technol.*, 60 (2014), 124.
- [6] BALU T., RAJASEKARAN T.R., MURUGAKOOTHAN P., *Physica B*, 404 (2009), 1813.
- [7] MOITRA S., KAR T., *Mater. Chem. Phys.*, 117 (2009), 204.
- [8] ANIS M., MULEY G.G., RABBANI G., SHIRSAT M.D., HUSSAINI S.S., *Mater. Technol. Adv. Perform. M.*, 30 (2015), 129.
- [9] KHANDPEKAR M.M., DONGARE S.S., PATIL S.B., PATI S.P., *Opt. Commun.*, 285 (2012), 1253.
- [10] ANIS M., MULEY G.G., SHIRSAT M.D., HUSSAINI S.S., *Cryst. Res. Technol.*, 50 (2015), 372.
- [11] PANDIAN M.S., BALAMURUGAN N., BHAGAVAN-NARAYANA G., RAMASAMY P., *J. Cryst. Growth*, 310 (2008), 4143.
- [12] PANDIAN M.S., RAMASAMY P., *J. Cryst. Growth*, 310 (2008), 2563.
- [13] PABITHA G., DHANASEKARAN R., *Mater. Sci. Eng. B-Adv.*, 177 (2012), 1149.
- [14] PANDIAN M.S., RAMASAMY P., *J. Cryst. Growth*, 312 (2010), 413.
- [15] KURTZ S.K., PERRY T.T., *J. Appl. Phys.*, 39 (1968), 3798.
- [16] XU D., LIU M.-G., HOU W.-B., YUAN D.-R., JIANG M.-H., REN Q., CHAI B.H.C., *Mater. Res. Bull.*, 29 (1994), 73.
- [17] MANSOOR S.-B., SAID A.A., WEI T.-H., DAVID J. HAGAN, STRYLAND VAN E.W., *IEEE J. Quantum Elect.*, 26 (1990), 760.
- [18] ANIS M., MULEY G.G., HAKEEM A., SHIRSAT M.D., HUSSAINI S.S., *Opt. Mater.*, 46 (2015), 517.
- [19] ANIS M., SHIRSAT M.D., MULEY G., HUSSAINI S.S., *Physica B*, 449 (2014), 61.
- [20] MAJOR A., AITCHISON J.S., SMITH P.W.E., DRUON F., GEORGES P., VIANA B., AKA G.P., *Appl. Phys. B*, 80 (2005), 199.
- [21] JIN L.T., WANG X.Q., REN Q., CAI N.N., CHEN J.W., LI T.B., LIU X.T., WANG L.N., ZHANG G.H., ZHU L.Y., XU D., *J. Cryst. Growth*, 356 (2012), 10.
- [22] GU B., HUANG X.Q., TAN S.Q., WANG M., JI W., *Appl. Phys. B*, 95 (2009), 375.
- [23] KUMAR S.S.R., RAO V.S., GIRIBABU L., RAO N.D., *Chem. Phys. Lett.*, 447 (2007), 274.
- [24] SRINIVASAN P., NOORALDEEN A.Y., KANAGASEKARAN T., DHINAA A.N., PALANISAMY P.K., GOPALAKRISHNAN R., *Laser Phys.*, 18 (2008), 790.
- [25] GIRISUN S.T.C., DHANUSKODI S., MANGALARAJ D., PHILLIP J., *Curr. Appl. Phys.*, 11 (2011), 838.
- [26] KUMAR A.R., VIZHI E.R., VIJAYAN N., BHAGAVAN-NARAYANA G., BABU R.D., *J. Pure Appl. Indian Phys.*, 1 (2010), 61.
- [27] ANUSHA P.T., REETA S.P., GIRIBABU L., TEWARI S.P., RAO V.S., *Mater. Lett.*, 64 (2010), 1915.
- [28] ANIS M., MULEY G.G., SHIRSAT M.D., HUSSAINI S.S., *Mater. Res. Innov.*, 19 (2015), 338.
- [29] SHAIKH R.N., ANIS M., SHIRSAT M.D., HUSSAINI S.S., *J. Optoelectron. Adv. M.*, 16 (2014), 1147.

Received 2015-10-25

Accepted 2016-05-27